Geologie en Mijnbouw **77:** 63–76, 1999.

Petrography and geochemistry of septarian carbonate concretions from the Boom Clay Formation (Oligocene, Belgium)

M. De Craen [1,2], R. Swennen [1] & E. Keppens [3]

[1] *Katholieke Universiteit Leuven, Fysico-chemische geologie, Celestijnenlaan 200C, B-3001 Heverlee, Belgium;* [2] *present address: SCK · CEN, Boeretang 200, B-2400 Mol, Belgium;* [3] *Vrije Universiteit Brussel, Dienst Geochronologie, Pleinlaan 2, B-1050 Brussels, Belgium*

Received 20 September 1995; accepted in revised form 9 September 1998

Key words: bacterial sulphate reduction, early diagenesis, geochemistry, stable isotopes

Abstract

The septarian carbonate concretions from the Boom Clay (Belgium) consist mainly of authigenic minerals such as micrite ($\leq$ 70% bulk volume) and pyrite framboids ($\backsim$ 3%). These mineral phases occur between detrital grains and fossils. The septarian cracks are lined with calcite, which is sometimes covered with pyrite. The preservation of delicate sedimentological features in the concretion matrix (hardly compacted faecal pellets, burrows and uncrushed shells) points to an early origin of the concretions. Systematic geochemical variations from concretion centre to edge suggest that growth continued during shallow burial. The $\delta^{13}C$ values (–17.5 to –20.5‰) of the concretionary carbonate show that bacterial sulphate-reduction processes were dominant. Sulphate-reduction-derived HCO_3^- was diluted by marine-related HCO_3^-, derived from dissolved bioclasts. A slight enrichment in $\delta^{13}C$ during growth is caused by the decreasing influence of sulphate reduction because of the progressive closure of the diagenetic system due to shallow-burial compaction. The $\delta^{18}O$ values (–0.5 to +1.0‰) of the concretionary carbonate point to a marine origin. The slightly ^{18}O-depleted signature with respect to time-equivalent marine-derived carbonate relates to the incorporation of an ^{18}O-depleted component, originating from sulphate and organic matter. The slight decrease in $\delta^{18}O$ during growth relates to an increasing influence of this component and to a decreasing influence of seawater-derived oxygen during early diagenesis.

Introduction

Organic-rich marine deposits are characterised by a sequence of depth-related diagenetic zones (Irwin et al. 1977, Irwin 1980, Coleman 1985, Curtis 1987, Dix & Mullins 1987, Raiswell 1987, Clayton 1992, Winter & Knauth 1992). Within each zone specific diagenetic processes occur of which degradation of the primary organic matter is one of the most important. Bicarbonate production can induce carbonate precipitation. The isotopic composition of these carbonates reflects the organic processes by which they have been formed. Changes in elemental and isotopic compositions within carbonate concretions in marine sediments may record changes in pore-water chemistry during their growth (Hudson 1978).

This paper aims to discuss the genesis of carbonate concretions in the Oligocene Boom Clay Formation in Belgium, and to report on subtle shifts in $\delta^{13}C$ and $\delta^{18}O$ signatures which reflect variations in C and O sources during concretion growth. In the Boom Clay, more than 10 closely spaced concretion-bearing horizons are present which can be correlated over several tens of kilometres (Vandenberghe & Laga 1986). This correlation is based on differences between the concretions of different horizons in shape, size, composition and cementing phases within the septarian cracks. The burial depth never exceeded 130 m (Vandenberghe & Laga 1986). Therefore, burial-diagenetic overprinting can be excluded. This paper discusses data from concretions of septaria horizon 40 (henceforth called S40) which is considered representative for most septaria horizons in the deposit.

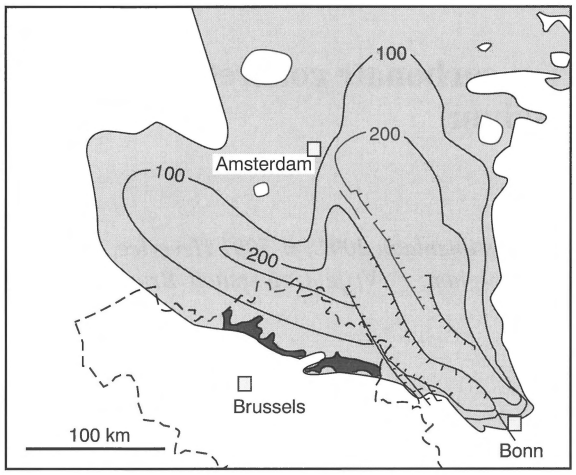

Figure 1. Simplified palaeogeographic map of the Rupelian sea north of Belgium, with schematic isopachs of the sediments (after Vinken 1988). Present-day outcrops of the Rupelian Boom Clay in Belgium are indicated in black.

The marine Boom Clay Formation (Rupelian, Lower Oligocene) crops out in northern Belgium (Figure 1). The formation, which can be up to 110 m thick (Mol borehole), consists of a cyclic sequence of silty clays and clayey silts with a rather constant chemical and mineralogical composition throughout (Vandenberghe 1978). A generalised section is shown in Figure 2A. The layering (Figure 2B) is the result of variations in grain size, carbonate content and organic-matter content, and reflects changes in local tectonics, eustacy and climate (i.e. Milankovitch cyclicity, Van Echelpoel & Weedon 1990, Van Echelpoel 1991). The layering is also reported in boreholes in the North Sea (Vandenberghe et al. in press) as well as in outcrops in NW Germany (Jung & Langer 1990).

Sampling and methodology

For a pilot study, S40 concretions were sampled from outcrops in the type area of the Boom Clay Formation, ca. 30 km north of Brussels (Figures 1, 2). Conventional, cathodoluminescence (CL), scanning electron (SEM) and backscattered electron microscopy (BSEM) were used for petrographic characterisation. Cathodoluminescence petrography was carried out with a Technosyn Cold Cathodo Luminescence Model 8200 Mk II (operating conditions: 16–20 kV, 420 μA gun current, 0.05 Torr vacuum and 5 mm beam width). SEM and BSEM research was conducted with a Jeol JSM 6400. In addition, thin sections were stained with Alizarine-Red-S and potassium ferrycyanide to differentiate between carbonate phases and to gather information on their relative iron content (Dickson 1966).

From three representative concretions a slab was taken from the middle part, in a direction normal to the bedding plane. Samples were then collected as shown in Figure 2D. They were subsequently crushed and analysed for:

- Concentrations of major and trace elements of bulk composition (after lithium-metaborate and HNO_3 dissolution and analysis by atomic emission spectrometry). Loss on ignition (LOI) was measured from 105 to 1000°C, while the insoluble residue (IR) was analysed gravimetrically after dissolution in HCl (0.5N).
- Concentrations of major and trace elements after 0.5N HCl dissolution (analysed by atomic absorption spectrometry).
- Stable carbon and oxygen isotopic compositions of the carbonate fraction. Samples were treated with anhydrous $\geq$100% orthophosphoric acid, using standard techniques after McCrea (1950). The results are reported in the δ-notation, relative to the PDB standard, for both carbon and oxygen (McCrea 1950). All data have been corrected for spectrometric analyses, based on the procedure of Craig (1957), and using repeated analyses of NBS-20 Solnhofen limestone (Coplen et al. 1983). Reproducibility, determined by replicate analysis, is better than $\pm$ 0.1‰ for oxygen and carbon at the 2σ level. Measurements were performed on a Finnigan Mat Delta-E stable isotope ratio mass spectrometer.

Field description and petrography

The septarian carbonate concretions in the Boom Clay always occur within thin bioclast-rich layers (Figure 2C). For S40, the present fossil content within the layer is about 15% but it differs from layer to layer. Preserved fossils mainly consist of coccoliths (Figure 3A); other fossils are foraminifera, ostracods, gastropods and bivalves. The layer displays a higher present-day porosity than the surrounding host sediment. This was most likely also the case after deposition. If so, such horizons may have acted as fluid conduits.

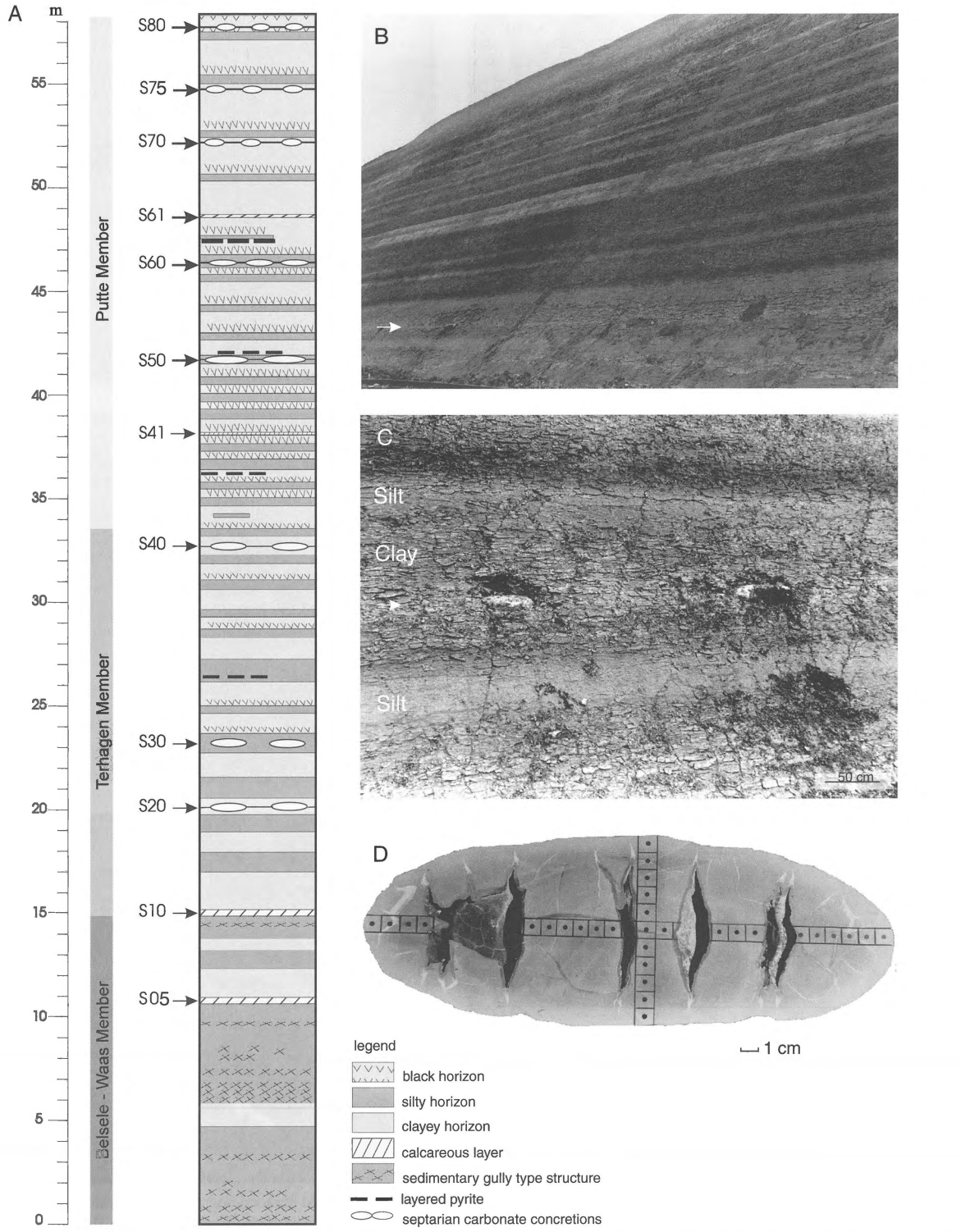

Figure 2. A) Composite lithostratigraphic column of the outcropping Boom Clay displaying the cyclic sequence of silty clays and clayey silts. S05 to S80 are septaria horizons (after Vandenberghe 1978). B) Cyclic alternation of silty clays (light grey in this photograph) and clayey silts (dark grey). Boom Clay quarry at Rumst, 30 km north of Brussels. Arrow indicates the carbonate-rich layer in which the S40 concretions occur. Height of photographed part of outcrop is ca. 16 m. C) S40 concretions occurring within a carbonate-rich layer (arrow) in the middle of a clayey horizon. See also Figure 2B. D) S40 concretion sawed normal to bedding, illustrating the flattened spheroidal shape and the calcite-lined, partly open septarian cracks. Subsamples for geochemical analysis were taken as indicated: carbon and oxygen isotopic analysis, □ subsamples of 1 cm^3 for major and trace element analysis.

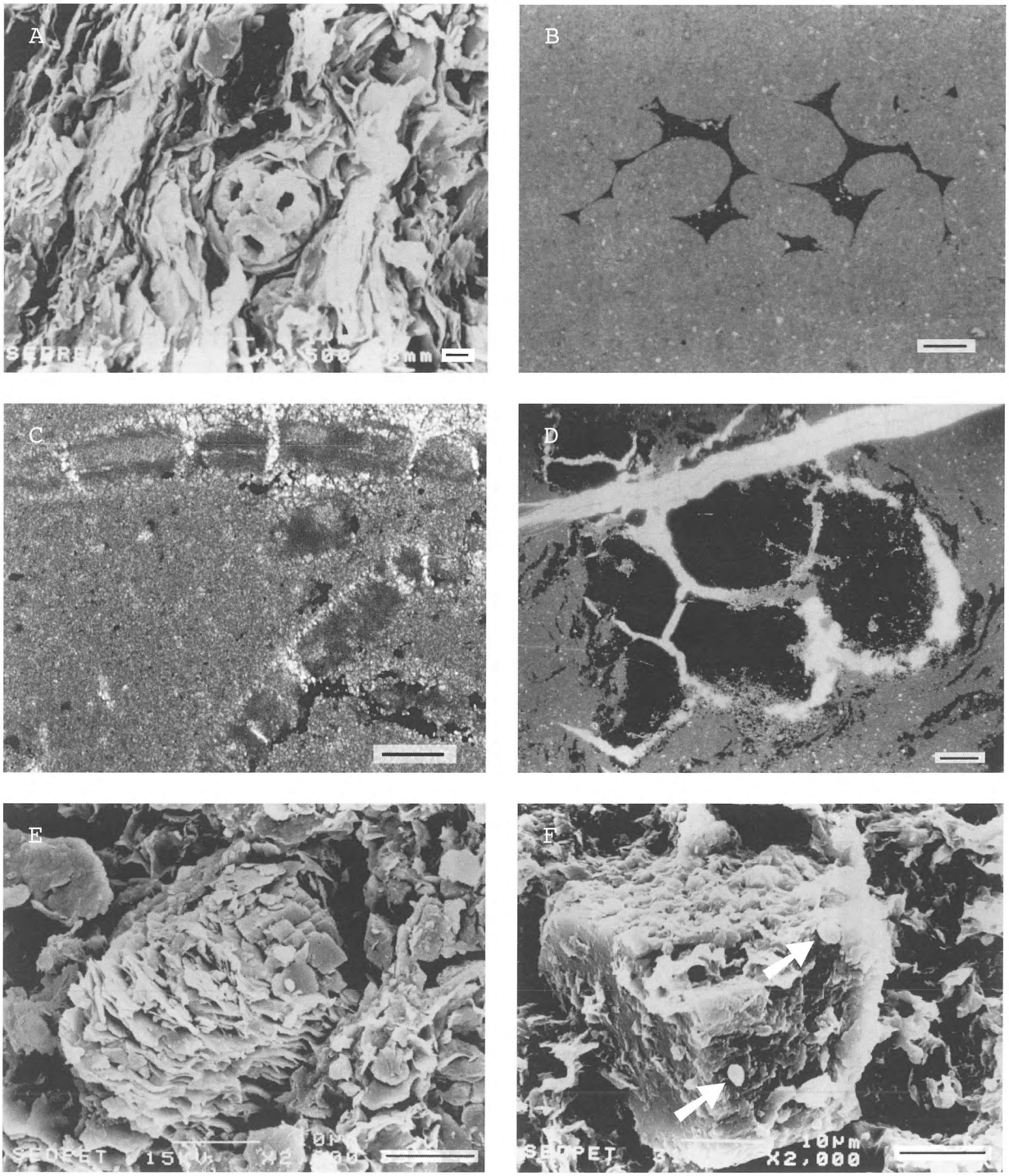

Figure 3. Petrography of S40 concretions from the Rupelian type locality at Rumst. A) SEM photomicrograph of carbonate-rich layer next to S40 concretions. Coccoliths create an open pore network within these otherwise rather compact clays. Scale bar = 1 μm. B) Photomicrograph of well-preserved faecal pellets within the concretion. Note the uncompacted to slightly compacted nature of the pellets. Framboidal pyrite is present between the pellets. Scale bar = 300 μm. C, D) Photomicrographs testifying to displacive concretion growth. Fossil shells (C) as well as pyrite nodules (D) are disrupted and the created open space is cemented by sparite. This also illustrates the early-diagenetic nature of the pyrite. Scale bars (C) = 100 μm, (D) = 600 μm. E) SEM photomicrograph showing carbonate partly replacing a clay-rich faecal pellet. Scale bar = 10 μm. F) SEM photomicrograph of an HCl-etched sample showing several bacteria (arrows) upon a large calcite crystal. Scale bar = 10 μm.

Table 1. Variations in chemical composition across an S40 concretion of about 15 cm thickness from the Rupelian type locality at Rumst.

Bulk rock										Carbonate fraction					
SiO_2 (%)	Al_2O_3 (%)	Fe tot. (%) *	Fe_2O_3 (%)	FeO (%)	CaO (%)	MnO (%)	MgO (%)	LOI (%)	IR (%) (HCl 0.5 N insoluble)	Fe (ppm)	Mg (%)	Mn (ppm)	Sr (ppm)	Na (ppm)	K (ppm)
13.20	4.49	2.07	0.97	0.99	42.0	0.12	2.31	35.0	20.9	6150	0.92	767	541	284	1101
12.14	4.19	1.79	0.94	0.77	42.3	0.14	2.21	35.8	18.3	5009	0.85	827	503	281	1017
10.40	3.93	1.50	0.88	0.56	43.7	0.13	2.15	36.5	16.8	4191	0.90	770	500	288	1101
10.38	3.72	1.40	0.77	0.57	43.7	0.11	2.13	36.8	16.4	3978	0.89	720	484	275	1042
10.75	4.02	1.53	0.90	0.57	43.5	0.13	2.16	36.4	17.1	4359	0.91	767	506	298	1252
11.86	4.12	1.90	1.02	0.79	42.4	0.14	2.08	35.8	17.5	5400	0.87	802	509	286	1147
13.06	4.43	2.20	1.11	0.98	41.2	0.12	2.18	35.1	19.9	6900	0.92	752	563	293	1185

* Fe tot. = (Fe^{2+} + Fe^{3+}) recalculated to Fe_2O_3

In general, all septarian concretions in the Boom Clay have a flattened ellipsoidal shape (Figure 2D). Sedimentary laminae or concentric zones have not been observed in these concretions. All concretions consist of a fine-grained matrix of detrital components and fossils, tightly cemented with micrite and microspar. Clay minerals dominate, together with detrital quartz. Minor amounts of muscovite, glauconite, feldspars, collophane and iron-oxides (possibly oxidised pyrite) also occur, as do coccoliths, foraminifera, ostracods, gastropods, and double-shelled molluscs which are mostly in life position. Delicate shells are often well-preserved and do not show any significant compactional deformation. Burrows (< 2 mm in diameter) frequently occur. Faecal pellets are clearly visible (Figure 3B). They occur in small groups within the concretion matrix, especially in burrows, and they are hardly compacted. Framboidal pyrite is present throughout the concretion matrix. It also occurs as infillings in foraminifera, or concentrated in burrows (Figure 3B). Large solid shell valves are often disrupted, with sparry calcite filling the created spaces (Figure 3C). Similar textures develop in burrows and in small concretionary pyrite bodies (Figure 3D).

The relatively uncompacted nature of the pellets and the presence of paper-thin uncrushed shell fragments indicate that lithification was initiated before or during the initial stage of compaction. At this stage, the sediment had a high porosity so that the dominant lithification process was cementation. The disrupted solid parts (thick shells and small concretionary pyrite bodies) which occur in all orientations (also perpendicular to stratification), and which do not show any relationship to internal shrinkage, indicate that cementation was to a certain degree displacive. However, replacement of the sediment by carbonate also took place. This can be inferred from the replaced faecal pellets (Figure 3E) and also from the partly replaced detrital grains, such as quartz and feldspars. Based on the 0.5N HCl-insoluble residue, the detrital content is presently < 20% and indicates that replacement and/or displacement by carbonate were, apart from cementation, important processes.

In etched samples (1N HCl for 1 minute) fossil bacteria occur on carbonate minerals (Figure 3F). This probably indicates that bacteria played a role in the precipitation of carbonate minerals, a process that was also invoked by Folk (1993). Since Ca^{2+} attaches strongly to bacterial cell walls, these bacteria create local microenvironments where the Ca^{2+} concentration is enhanced. This may cause supersaturation with respect to calcite. Carbonate minerals will then crystallise within or around the bacteria. This suggests that bacteria are important in carbonate concretion growth.

Geochemistry

Apart from an outer, relatively clay-rich edge (± 1 cm thick), the internal matrix of S40 concretions seems homogeneous. Samples for geochemical analysis were taken each centimetre, in vertical and horizontal directions (Figure 2D). In both directions, systematic variations in elemental and isotopic composition occur from centre to edge. Since these compositional changes are similar for all directions, only data from one of the vertical sections are given in Table 1 and Figures 4 and 5.

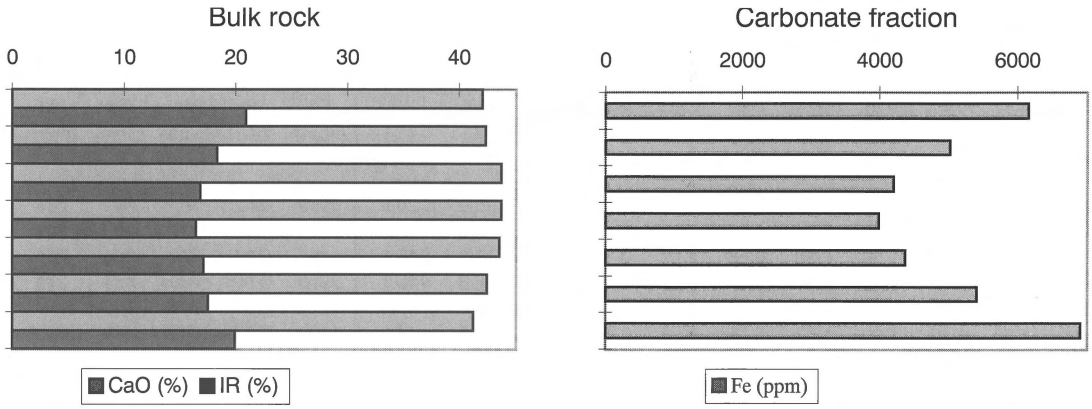

Figure 4. Variations in chemical composition across an S40 concretion of about 15 cm thickness from the Rupelian type locality at Rumst (full data in Table 1). A decrease in the CaO content of the bulk rock towards the concretion edges is coupled with an increase in SiO_2, Al_2O_3, Fe_2O_3 and IR. Within the carbonate fraction, Fe increases towards the edges.

Major and trace element composition

Table 1 and Figure 4 show the chemical variation across one S40 concretion. The carbonate content of the concretions (carbonate cement and bioclast relicts), measured as CaO, generally varies between 70 and 80%. A remarkable feature occurring in the three investigated S40 concretions is the systematic compositional variation from centre to edge. Similar trends in major and trace elements have been observed in other concretion horizons in the Boom Clay (De Craen 1998) as well as in other formations (Raiswell 1971, 1976, Curtis et al. 1975, 1986, Irwin 1980, Gautier et al. 1985, Mozley 1989, Scotchman 1991, Moore et al. 1992).

A decrease in the CaO content of the bulk rock towards the concretion edge is coupled with an increase in SiO_2, Al_2O_3, Fe_2O_3 and insoluble residue (IR). Within the carbonate fraction, Sr and Fe display an increasing trend towards the edge. This is also the case for Mn, although for this element concentrations decrease again in the outermost rim. No clear trend is recognisable for Mg, K and Na. However, the rather high content of the last two elements suggests that also leaching of K and Na from clays occurred. Since no covariance exists between K and Fe, and between Mn and Sr, Fe and Sr contents mainly relate to the carbonate fraction.

These variations are interpreted in terms of concretion growth during burial. Burial causes a decrease in the pore space available for carbonate cementation. The content of detrital minerals, reflected in the patterns of SiO_2, Al_2O_3, Fe_2O_3 and IR, thus increases from concretion centre to edge. The increase in Fe and partly also in Mn in the carbonate fraction reflects an evolution towards increasing reducing conditions.

These trends confirm the petrographic observations, namely that concretion growth was initiated during very early diagenesis within the first metres of burial, and continued during shallow burial.

Carbon and oxygen isotope composition

The stable carbon isotopic composition of the three investigated S40 concretions varies between –17.5 and –20.5‰. A progressive enrichment in ^{13}C from concretion centre to edge is observed, with a reversal in the outermost, relatively clay-rich part (Figure 5). The $\delta^{18}O$ values vary between –0.5 and +1‰ and show a depletion in $\delta^{18}O$ from centre to edge, with a reversal in the outer part (Figure 5).

The isotopic signatures of the S40 concretions and the evolution of these signatures during concretion growth can only be explained by considering different sources. For carbon these sources are: seawater HCO_3^-, HCO_3^- derived from the bacterial degradation of organic matter (sulphate reduction, methanogenesis), HCO_3^- derived from the oxidation of upward diffusing methane, and HCO_3^- derived from the dissolution of fossils. Oxygen sources are: seawater (H_2O, HCO_3^-, SO_4^{2-}), HCO_3^- derived from the bacterial degradation of organic matter and HCO_3^- derived from the dissolution of fossils.

Carbon

Light carbon isotopic values are generated during bacterial oxidation, microbial ferric iron reduction and bacterial sulphate reduction (Irwin et al. 1977, Irwin 1980). The light carbon isotopic signature of the

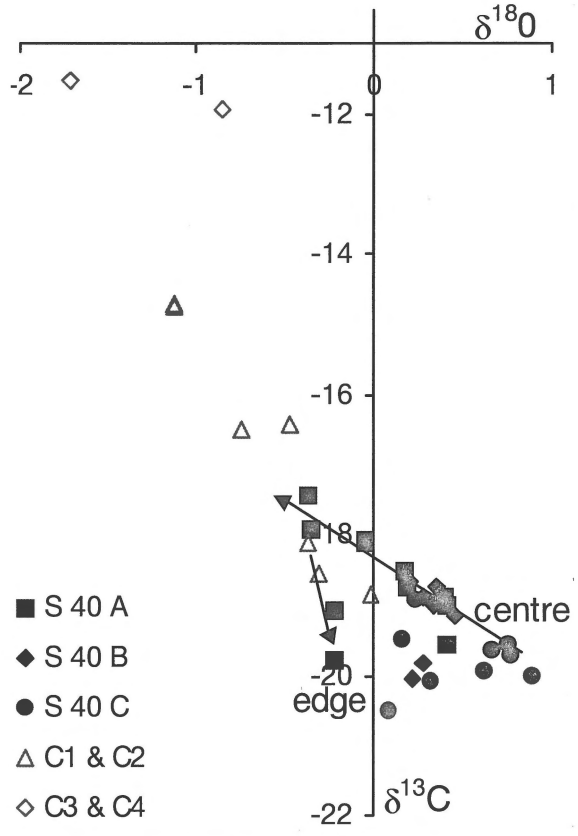

Figure 5. Variation in carbon and oxygen isotopic composition of three representative S40 concretions from the Rupelian type locality at Rumst. The arrow shows the evolution of the isotopic composition from centre to edge of the S40A concretion. A similar evolution is present in the other concretions. The isotopic composition of the septarian cements is also shown.

S40 concretions, between –17.5 and –20.5‰, its limited range, the inferred presence of sulphate-reducing bacteria, and the widespread presence of framboidal pyrite, indicate that the S40 concretions formed mainly or entirely within the sulphate-reduction zone, with major HCO_3^- contribution from degradation of organic matter by sulphate-reducing bacteria (Irwin et al. 1977, Irwin 1980, Coleman & Raiswell 1981, Raiswell 1987). However, mixing with less ^{13}C-depleted HCO_3^- must have occurred in the S40 concretions, since the carbon isotopic composition is slightly more enriched in comparison to the –25‰ value which is typical for the sulphate-reduction zone. Bioclasts occurring within the concretions, might explain this relative enrichment. However, their content which is estimated to vary around 1% of the bulk rock volume, is too low to explain the observed isotopic shift. HCO_3^- derived from dissolved aragonitic material from the bioclast-rich layers, in which the concretions occur, forms a likely alternative source. Neither can HCO_3^- derived from methanogenesis be excluded. However, it is unclear whether the influx of methanogenic HCO_3^- would allow to maintain the $\delta^{13}C$ within the limited range recorded in the concretions.

The changes in stable carbon isotope composition in the S40 concretions may be explained in several ways:

1) *Transition from sulphate reduction to methanogenesis.* Sulphate-reduction processes generate HCO_3^- with a ^{13}C-depleted carbon isotope composition. As burial proceeds, the sediment reaches the methanogenesis zone, where isotopically light CH_4 and isotopically heavy HCO_3^- are produced. Increasing contribution of the isotopically heavy HCO_3^- can explain a trend towards ^{13}C enrichment. Methanogenesis, however, is usually considered to be of limited importance in the Boom Clay, but it can be invoked to explain the observed trend in $\delta^{13}C$ in the S40 concretions.
2) *Changes in sulphate-reduction process, organic matter or bacteria.* Changes in $\delta^{13}C$ of the produced concretionary carbonate can occur as a function of the type of organic matter species that is altered through time. It is likely that, during the initial stages of sulphate reduction, the easily degradable types of organic matter will be affected first. As time proceeds, other less easily degradable types of organic matter will be affected. This may result in a change in the carbon isotope signature, depending on the original isotope composition of the oxidised organic matter. Moreover, if different types of sulphate-reducing bacteria are involved, different isotopic fractionations may occur. This is directly related to the dominant sulphate-reduction process (Claypool & Kvenvolden 1983). Unfortunately, insufficient information is available to evaluate this possibility.
3) *Variations in the relative contributions of marine-derived and sulphate-reduction-derived carbon.* Local differences in sedimentology (such as type and amount of reactive organic matter, bioclasts, ...) and changes in sedimentological and concomitant early-diagenetic conditions during shallow burial cause changes in the relative contributions of carbon derived from different sources. In our opinion, this is the most important process causing the observed trend in the S40 concretions. During shallow burial, the diagenetic system changes

from open to semi-closed or closed, and thus the replenishment of the sediment's pore-water with seawater sulphate decreases. This occurs before methanogenesis might start to interfere. The amount of SO_4^{2-} available for reduction decreases and thus the sulphate-reduction process becomes hampered. Consequently, a decrease in the contribution of sulphate-reduction-related HCO_3^- occurs, which results in a slight enrichment of ^{13}C. The systematic trend reversal at the edge of the S40 concretions indicates that a ^{13}C-depleted HCO_3^- source becomes more important. Possibly, a depletion of the amount of easily dissoluble bioclasts can explain the trend reversal.

Oxygen

The $\delta^{18}O$ values are lower than those expected from reported Oligocene marine components. These reported $\delta^{18}O$ values vary between +1.0 and +2.5‰ (Shackleton 1986). Analysed bioclasts of the Boom Clay (*Nucula* shells, gastropods) indeed display $\delta^{18}O$ values between +1.5 and +2.1‰. A depletion with respect to marine water has previously been explained by Sass et al. (1991) as a result of the incorporation of ^{18}O-depleted oxygen from sulphate and organic matter into the pore-water bicarbonate. Very recently, such a mechanism has been proved by laboratory experiments, carried out by Mortimer & Coleman (1997), who showed that $\delta^{18}O$ values of early-diagenetic marine carbonates are anomalously low due to microbial influences. Nevertheless, the $\delta^{18}O$ values of the S40 concretionary carbonates are still compatible with an early initiation of concretion growth, close to the sediment/water interface. Similar observations were made by Raiswell (1976), Hudson (1978), Pearson (1979), Coleman & Raiswell (1981), Thyne & Boles (1989) and others.

Mozley & Burns (1993) recently invoked several mechanisms to explain ^{18}O-depletion trends in marine carbonate concretions. Based on the previous observations, one or more of the following processes can be invoked for the Boom Clay concretions:

1) *Increasing precipitation temperatures.* Oxygen isotope fractionation between water and carbonate is strongly temperature-dependent. Lower $\delta^{18}O$ values are associated with higher precipitation temperatures (Veizer 1992, Hoefs 1997). By accepting a constant water composition and using the palaeotemperature equation of Craig (1965; modified after Epstein et al. 1953), the isotopic shift from concretion centre to edge reflects a temperature increase of about 3.8°C. This corresponds to concretion growth over a 130 m interval (accepting a geothermal gradient of 3°C/100 m). This is in the order of the maximum burial depth of the Boom Clay in the Rupel area. As stated before, concretion growth started within the sulphate-reduction zone and clear evidence that growth continued in the zone of methanogenesis is absent. The lower limit of the sulphate-reduction zone is determined by the balance between SO_4^{2-} diffusing down from the depositional waters and SO_4^{2-} consumption by bacteria (Curtis 1987), and most typically reaches to 10 m depth (Coleman & Raiswell 1981; Dix & Mullins 1987). However, it is doubtful whether sulphate reduction in our case reached down to a depth of > 100 m. The ^{18}O-depletion is thus enhanced by other processes.

2) *Recrystallisation or influx of meteoric water during the Late Rupelian-Chattian emersion.* In the S40 concretions, the concretionary carbonate shows similar CL and SEM characteristics from centre to edge, and microfabrics and concentric geochemical variations are preserved. Neither dissolved or corroded crystals, nor the development of zoned cements have been observed. Thus no evidence for recrystallisation or meteoric alteration is present. Furthermore, these processes cannot explain the trend reversal in oxygen isotopic composition at the concretion edge.

3) *Water/mineral interactions.* Interaction of the pore-water with authigenic clay minerals, resulting from the alteration of volcanic material which is present in the Boom Clay (Zimmerle 1991, 1993), can explain the depletion in ^{18}O.

4) *Incorporation of ^{18}O-depleted oxygen derived from sulphate and organic matter.* ^{18}O-depleted oxygen isotope compositions of carbonates can reflect the diagenetic modification of pore-water due to bacterial oxidation of organic matter by sulphate (Coleman & Raiswell 1981, Sass et al. 1991, Mortimer & Coleman 1997). Isotopically light oxygen is derived both from sulphate and organic matter. During shallow burial, the diagenetic system becomes gradually more closed with respect to seawater and seawater sulphate. Consequently, the sulphate-reduction process will slow down and the influence of oxygen derived from organic matter or sulphate decreases with time. The

observed ^{18}O-depletion thus cannot be explained by the sulphate-reduction process.

Estimated concretion growth rates

The cyclic sedimentation of the Boom Clay Formation is controlled by orbital, climatological forces (Van Echelpoel 1991). Based on the assumption that either the 41 ka obliquity or the 100 ka eccentricity was the dominant controlling process, an average sedimentation rate of 2.44 or 1.00 m/100 ka, respectively, can be calculated. According to N. Vandenberghe (pers. comm.) the 100 ka eccentricity process was probably dominant, since in that case the Boom Clay Formation represents about 80% of the sedimentation record over the whole time period of about 5 Ma. If concretion growth happened over the 'typical' depth of the sulphate-reduction zone, i.e. down to 10 m (Coleman & Raiswell 1981, Dix & Mullins 1987), a minimum concretion growth rate of an S40 concretion with a total volume of 10 000 cm^3 can be calculated. In the obliquity-controlled and the eccentricity-controlled cyclicity scenarios, concretion growth would be in the order of 24.4 and 10 mm^3/a, respectively. This is equivalent to 0.66×10^{-3} and 0.27×10^{-3} mol $CaCO_3/a$, respectively. Obviously, these values only indicate an order of magnitude and would change according to variations in concretion-growth duration (i.e. depth).

Septarian cracks

All concretions in the Boom Clay show a typical septarian cracking pattern (Figure 2D). The cracks are at their widest in the centre and narrow towards the concretion margins. They never reach the concretion surface. Vertical cracks are better developed than horizontal ones. The cracks, of which the larger ones are open, are lined with several generations of fibrous calcite cement and/or cuboctahedral pyrite, several tens of microns in size. The cracks either cut through fossil shells or follow the fossil outline. The cracked fossils reflect advanced cementation of the concretion at the time of cracking. In the second case, the fossils are pulled out of the surrounding sediment on one side, where a mold remains. In this case, the fossils were not cemented with their surrounding sediment. This is frequently observed towards the edges of the concretions. Here tapering flakes of concretion material occur at both sides of the cracks (Figure 6A). Similar flakes have been described by Hesselbo & Palmer (1992). They resemble structures created by cracking of stiff Boom clay (Figure 6B). Cracks near edges tend to be curved in contrast to the vertical rectilinear cracks in the centres of the concretions.

These observations suggest that, at the time of cracking, the core of the concretion was well cemented so that brittle cracks developed, which may cross-cut fossil shells, etc. The outer parts were not entirely cemented and had both brittle and plastic characteristics. Here, flakes and curls of the concretion matrix developed within the cracks and fossils were pulled out of their surroundings. At the outermost edge, the partly cemented sediment was still very clay-rich and plastic, allowing gradual disappearance of the cracks.

Septarian cracks are characteristic of highly porous sediments (Raiswell 1971). Richardson (1919), Lippman (1955), Berner (1968) and Raiswell (1971) noted that dewatering of the originally plastic or gel-like concretion centre caused shrinkage cracks with a characteristically hexagonal pattern. Hudson & Friedman (1974), Duck (1995) and Mostefaï (1996) also favoured the idea that septarian cracks formed by dewatering of the concretion matrix. Astin (1986), however, suggested that the cracks formed as tensile fractures during burial and compaction of the host sediment. Physical compactional stresses, causing overpressuring in the enclosing mudrock, would result in tensional failure of concretions. In the absence of extensional tectonics (low horizontal stresses), septarian cracking would require raised pore-fluid pressures to form. This could be achieved during rapid burial, when sediment compaction is so fast that pore-fluids cannot escape. Sedimentation rates for the Boom Clay, calculated by Van Echelpoel (1991) are in the order of 1.00 to 2.44 m/100 ka. Whether these moderate rates were high enough to generate the overpressuring of Astin's interpretation is difficult to evaluate. Recently, Hounslow (1997) argued that septarian cracks form as a result of tensional failure due to local excess pore-fluid pressure inside the concretions, in normally consolidating mudrocks. This excess pressure is caused by the permeability reduction initiated by cementation.

Septarian crack cements

The septarian cracks are lined with a brown calcite. This colour could be due to inclusions of organic matter (Scotchman 1991) or dispersed oxidised Fe.

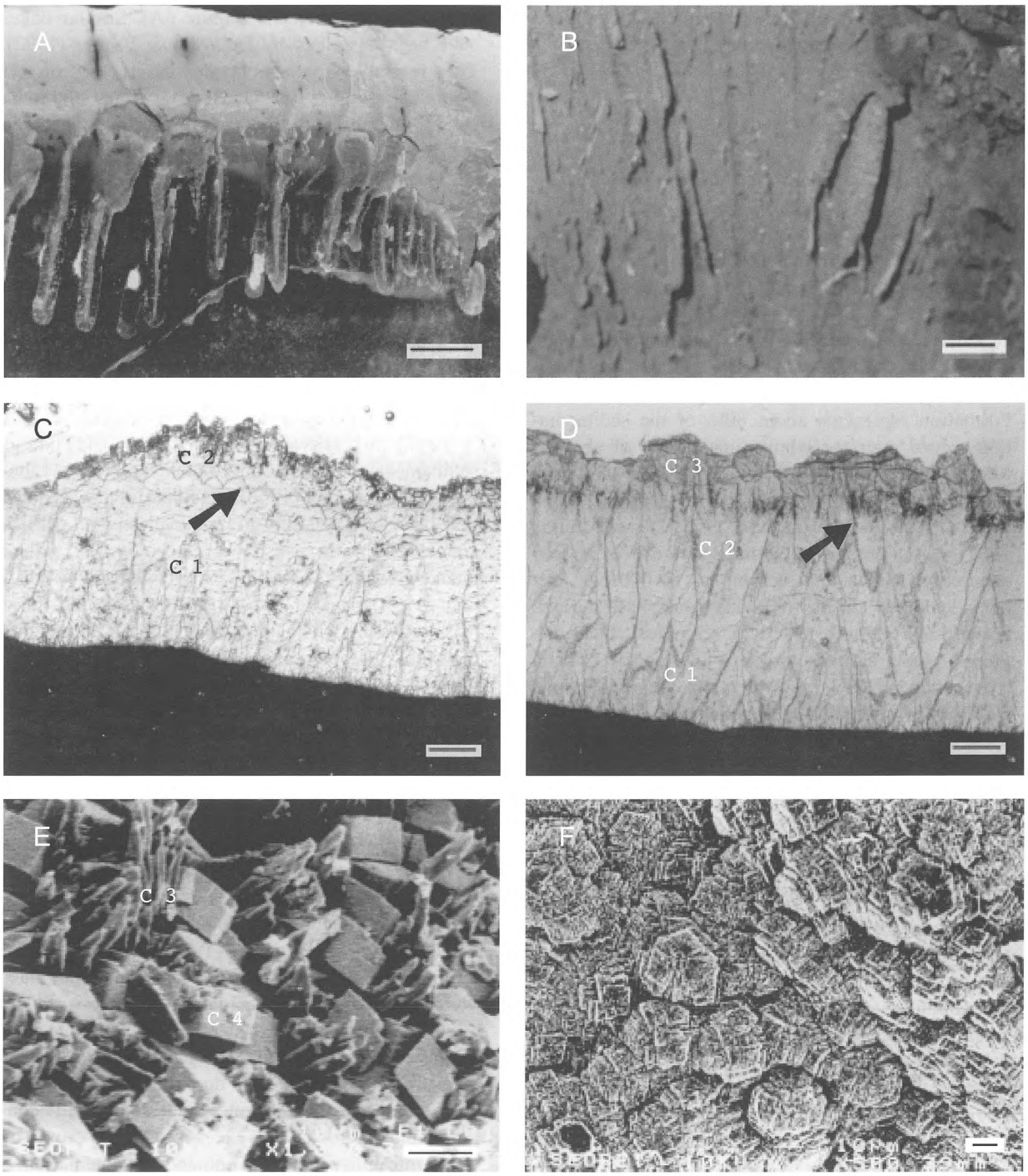

Figure 6. Septarian cracks and cements in S40 concretions from the Rupelian type locality at Rumst. A) Macroscopic view of a crack wall in the outer part of an S40 concretion, with tapering flakes of concretion material cemented by calcite. Development of the flakes reflects plastic behaviour of the concretion at the time of cracking. Scale bar = 1 cm. B) Development of tapering flakes within outcropping stiff Boom Clay fractured today. These are comparable to the flakes present within cracks which occur in the outer parts of the concretions (Figure 6A). Scale bar = 1 cm. C) Photomicrograph showing the first generation of radiaxial fibrous calcite cement, C1. The overgrowing fibrous calcite cement, C2, is slightly more ferroan, and is in optical continuity with C1. Note also the exceptionally well developed crystal terminations of C1 (arrow). Scale bar = 100 μm. D) Photomicrograph showing the conical nature of the C1 cements. The first two calcite generations cannot be distinguished without staining or CL microscopy. The inclusion-rich zone (arrow) marks the contact between C2 and C3 calcite cement. The latter is characterised by its fibrous and conical texture and its brown colour. The irregular outer surface is due to sample preparation. Scale bar = 100 μm. E) SEM photomicrograph of rhombohedral calcite crystals (C4) upon fibrous calcite (C3). Scale bar = 10 μm. F) SEM photomicrograph illustrating another aspect of the rhombohedral calcite cement (C4). Scale bar = 10 μm.

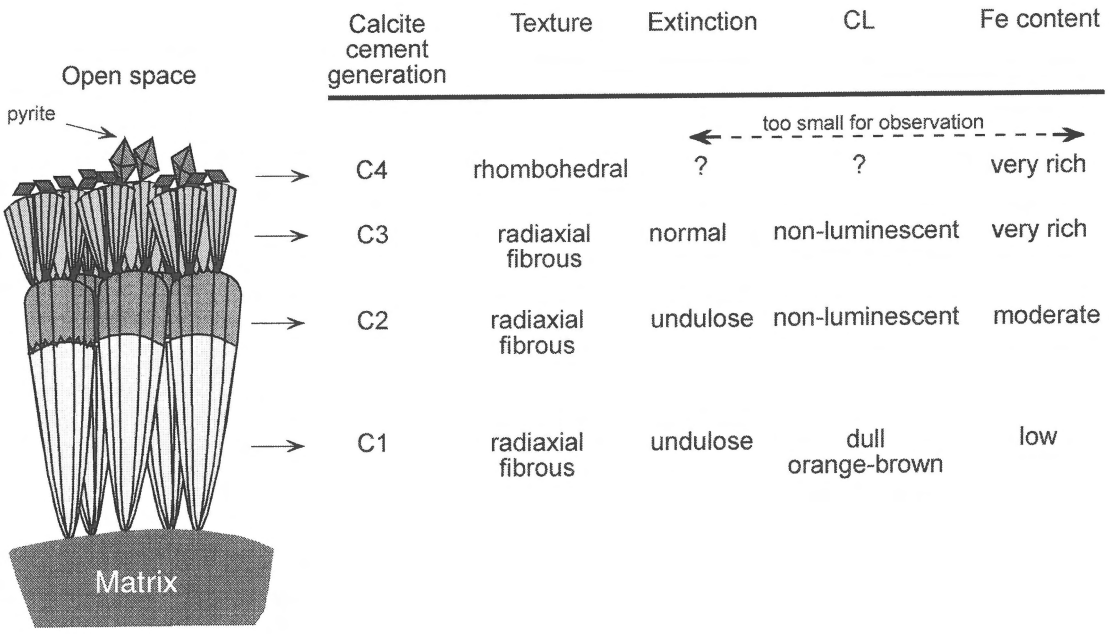

Figure 7. Schematic representation of the cement generations C1 to C4 filling the septarian cracks. Thickness of cement lining in open cracks is up to 0.5 cm.

The calcite cement consists of different generations (Figures 6A–D). Their petrographic characteristics are shown in Figure 7. Growth of the first cement generation, C1, was often initiated on an apex on which bundles of fibrous crystals grew (radiaxial fibrous cement). Close to the crack wall, a lot of inclusions are present, mainly consisting of small fragments of the concretion matrix. Well-defined crystal terminations, like those shown in Figure 6C, are present exceptionally. A second cement generation, C2, occurs as overgrowth cement. It is in optical continuity with the first generation. This cement, however, stains blue, pointing to a higher Fe content. In between the C2 calcite and the third cement generation, C3, an inclusion-rich zone occurs (Figure 6D). The fibrous C3 cement displays a brownish hue in thin section and is strongly ferroan and nonluminescent. It consists of different divergent cones. A fourth cement generation, C4, has only been identified under SEM. It consists of rhombohedral calcite crystals occurring on top of the C3 cones (Figures 6E, F). Subsequently, octahedral pyrite may occur.

The C1 calcites are identical to the cone structures described by Marshall (1982). Kendall & Tucker (1973) interpreted similar radiaxial fibrous calcite phases as replacement of precursor acicular calcite cements. However, Kendall (1985) later reinterpreted these radiaxial fibrous calcite cements as being primary in origin. The radiaxial texture results from split-crystal growth which is commonly caused by crystal poisoning. The septarian cements within the S40 concretions are also interpreted as being primary in origin, since acicular relict textures have not been observed. Recrystallisation also would have caused a homogenisation of the chemical composition of C1 and C2. However, a rather distinct difference in Fe content exists between these cement generations. This increase in Fe content, which concurs with an evolution in CL characteristics from dull to nonluminescent, reflects an evolution towards increasing reducing conditions. A similar evolution can be inferred from the stable isotopes.

The carbon and oxygen isotopic data of the calcite cements in various concretions (not specified) are shown in Figure 5. Unfortunately, it was not possible to sample the four generations separately. Values of the earliest fibrous calcites (C1 and C2) vary from –18.87 to –14.69‰ for $\delta^{13}C$ and from –0.02 to –1.12‰ for $\delta^{18}O$. These values are comparable to the isotopic composition of the concretion matrix. It can therefore be concluded that precipitation of C1 and C2 occurred from marine-related fluids within the sulphate-reduction zone. According to petrographic observations, this happened when the concretion was

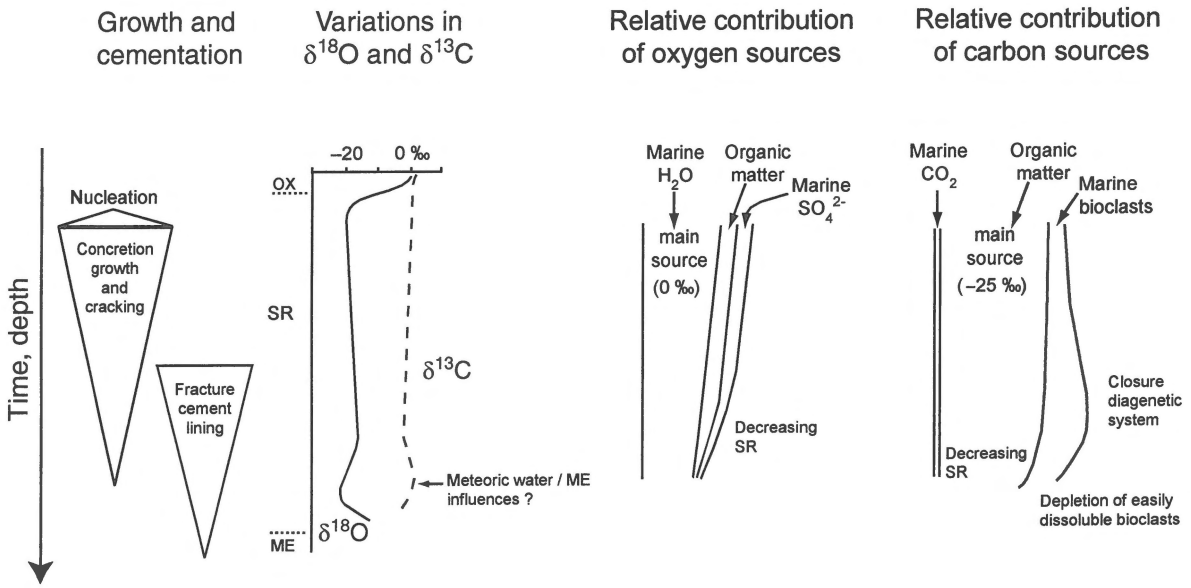

Figure 8. Schematic representation of concretion growth during burial with emphasis on the evolution of the contributing sources of different carbon and oxygen isotopes. OX = oxidation zone; SR = sulphate-reduction zone; ME = methanogenesis zone.

in its final stage of growth. The general trend to less depleted $\delta^{13}C$ and more depleted $\delta^{18}O$ continues in the ferroan calcite cement phases C3 and C4. They possess $\delta^{13}C$ values of –11.94 and –11.52‰ and $\delta^{18}O$ values of –0.85 and –1.72‰. Such an evolution towards less depleted $\delta^{13}C$ and more depleted $\delta^{18}O$ values reflects cementation during progressive shallow burial down to the transition zone from sulphate reduction to methanogenesis (Irwin et al. 1977).

Conclusions

The Boom Clay Formation contains several horizons in which septarian carbonate concretions occur. Based on petrographic and geochemical studies of the S40 horizon, a representative example for these horizons, a model for concretion growth with an emphasis on the evolution in isotopic signature is proposed in Figure 8. The following conclusions can be drawn:

1) Stable carbon and oxygen isotopic data ($\delta^{13}C$ between –17.5 and –20.5‰, $\delta^{18}O$ between +1 and –0.5‰) indicate that the concretions formed early in diagenesis, under anoxic conditions, close to the sediment/water interface and within the zone of sulphate reduction. Minor influences of methanogenesis, however, cannot be excluded. Early diagenetic growth, before significant compaction, is also indicated by the preservation of delicate sedimentological features, such as uncompacted faecal pellets and uncrushed paper-thin shells.
2) The concretions formed due to carbonate precipitation in the pores of the sediment. The Ca^{2+} is mainly derived from the dissolution of aragonitic skeletal material, while the HCO_3^- originated both from such material and from bacterial reactions degrading organic matter. Disrupted shells, pyrite nodules and stretched burrows indicate that cementation was partly displacive. Replacement of the sediment by carbonate also occurred, as proved by the replaced faecal pellets and by relicts of detrital grains which were partly replaced by carbonate. The existence of few intensively corroded detrital grains which are dispersed within the matrix suggests that replacement was pervasive.
3) Systematic changes in major and trace elements occur from concretion centre to edge, and reflect the evolving pore-water geochemistry during shallow burial. The increase of Fe and Mn contents in the carbonate fraction is interpreted in terms of the evolution from suboxic to reducing pore-waters.
4) The $\delta^{18}O$ values of the concretionary carbonate are slightly lower than expected for carbonate precipitation in equilibrium with Oligocene marine water. This discrepancy is explained by microbial influences, namely incorporation of ^{18}O-depleted

oxygen derived from organic-matter degradation and sulphate reduction under reducing conditions (Sass et al. 1991, Mortimer & Coleman 1997).

5) The isotopic signature of the concretions and the evolution of this signature during concretion growth can only be explained considering different sources. Gradual closure of the diagenetic system results in changes in the relative contribution of marine-derived and bacterial-derived carbon and oxygen, resulting in a ^{13}C enrichment and ^{18}O depletion.
6) The septarian cracks developed during concretion growth. Cracking occurred when the concretion core was already cemented. In the outer concretion zones, which were both brittle and plastic, tapering flakes border the cracks. At the outermost edge, the partially cemented sediment reacted plastically and cracks became curved and gradually ended.
7) The septarian cracks, of which the larger ones are open, are lined with brown fibrous calcite cement. Four calcite cement generations can be recognised. They show an evolution towards higher Fe contents. Rhombohedral calcite cement and finally pyrite form the latest cement phases. The stable carbon and oxygen isotope ratios of the calcite cements are in line with the stable isotope trend recognised within the concretion body. Calcite cementation started in the sulphate-reduction zone and possibly ended at the transition from sulphate reduction to methanogenesis.

Acknowledgements

We especially thank N. Vandenberghe and Ph. Muchez for their critical comments and helpful suggestions on a draft of this paper. C. Moldenaers and H. Nijs are thanked for preparing the thin sections, D. Coetermans for carrying out the major and trace element analysis, and P. Nielsen, J. Nijs and A. Van Riet for assisting with the stable isotope analysis. This research was partly supported by grants from the National Fund of Scientific Research of Belgium (project Nr 2.0038.91N).

References

Astin, T.R. 1986 Septarian crack formation in carbonate concretions from shales and mudstones – Clay Minerals 21: 617–631

Berner, R.A. 1968 Rate of concretion growth – Geoch. Cosmochim. Acta 48: 605–615

Claypool, G.E. & K.A. Kvenvolden 1983 Methane and other hydrocarbon gases in marine sediments – Ann. Rev. Earth planet. Sci. 11: 299–327

Clayton, C. 1992 Quantitative Diagenesis: Recent Developments and Applications to Reservoir Geology: Microbial and Organic Processes – NATO Advanced Study Institute for postdoctoral scientists and advanced students, University of Reading (England), 6-19/9/1992, 20 pp

Coleman, M.L. 1985 Geochemistry of diagenetic non-silicate minerals: kinetic considerations – Phil. Trans. R. Soc. London A315: 39–56

Coleman, M.L. & R. Raiswell 1981 Carbon, oxygen and sulphur isotope variations in concretions from the Upper Lias of NE England – Geochim. Cosmochim. Acta 45: 329–340

Coplen, C., C. Kendall & J. Hopple 1983 Comparison of stable isotope reference samples – Nature 302: 236–238

Craig, H. 1957 Isotope standards for carbon and oxygen mass-spectrometric analysis of carbon dioxide – Geochim. Cosmochim. Acta 12: 133–149

Craig, H. 1965 The measurement of oxygen isotope paleotemperatures. In: Tongiorgi, E. (ed.) Stable Isotopes in Oceanographic Studies and Paleotemperatures. Consiglio Naz. Rich., Lab. Geol. Nucleare, Pisa: 161–182

Curtis, C.D. 1987 Mineralogical consequences of organic matter degradation in sediment: Inorganic/organic diagenesis. In: Leggett, J.K. & G.G. Zuffa (eds) Marine Clastic Sedimentology. Graham and Trodman: 108–123

Curtis, C.D., M.J. Pearson & V.A. Somogyi 1975 Mineralogy, chemistry, and origin of a concretionary siderite sheet (clay-ironstone band) in the Westphalian of Yorkshire – Mineralogical Magazine 40: 385–393

Curtis, C.D., M.L. Coleman & L.G. Love 1986 Pore-water evolution during sediment burial from isotopic and mineral chemistry of calcite, dolomite and siderite concretions – Geochim. Cosmochim. Acta 50: 2321–2334

De Craen, M. 1998 The formation of septarian carbonate concretions in organic-rich argillaceous sediments – Unpubl. PhD thesis, K.U. Leuven, 330 pp

Dickson, J.A.D. 1966 Carbonate identification and genesis as revealed by staining – J. Sedim. Petrol. 36: 491–505

Dix, G.R. & H.T. Mullins 1987 Shallow subsurface growth and burial alteration of Middle Devonian calcite concretions – J. Sedim. Petrol. 57: 140–152

Duck, R.W. 1995 Subaqueous shrinkage cracks and early sediment fabrics preserved in Pleistocene calcareous concretions – J. Geol. Soc. London 152: 151–156

Epstein, S., R. Buchsbaum, H.A. Lowenstam & H.C. Urey 1953 Revised carbonate water isotopic temperature scale – Geol. Soc. Am. Bull. 64: 1315–1326

Folk, R.L. 1993 SEM imaging of bacteria and nannobacteria in carbonate sediments and rocks – J. Sedim. Petrol. 63: 990–999

Gautier, D.L., Y.K. Kharaka & R.C. Surdam 1985 Relationship of organic matter and mineral diagenesis – Soc. Econ. Paleontol. Mineral. short course 17: 1–36

Hesselbo, S.P. & T.J. Palmer 1992 Reworked early diagenetic concretions and the bioerosional origin of a regional discontinuity within British Jurassic marine mudstones – Sedimentology 39: 1045–1065

Hoefs, J. 1997 Stable Isotope Geochemistry, Fourth Edition. Springer Verlag, Berlin, 201 pp

Hounslow, M.W. 1997 Significance of localized pore pressures to the genesis of septarian concretions – Sedimentology 44: 113–1147

Hudson, J.D. 1978 Concretions, isotopes, and the diagenetic history of the Oxford Clay (Jurassic) of central England – Sedimentology 25: 339–370

Hudson, J.D. & I. Friedman 1974 Carbon and oxygen isotopes in concretions: relationship to pore water changes during diagenesis. In: Cadek, J. & T. Paces (eds) Proc. Internat. Sympos. Water-Rock Interaction, Czechoslovakia: 331–339

Irwin, H. 1980 Early diagenetic carbonate precipitation and pore fluid migration in the Kimmeridge Clay of Dorset, England – Sedimentology 27: 577–591

Irwin, H., C. Curtis & M. Coleman 1977 Isotopic evidence for source of diagenetic carbonates formed during burial of organic-rich sediments – Nature 269: 209–213

Jung, D. & W. Langer 1990 Foraminiferen aus dem Oligozän des Schachtes Lohberg IV bei Hünxe a. d. Lippe (Niederrheinische Bucht) – N. Jb. Geol. Paläont. Abh., 180: 75–96

Kendall, A.C. 1985 Radiaxial fibrous calcite: a reappraisal – Soc. Econ. Paleontol. Mineral. 36: 59–77

Kendall, A.C. & M.E. Tucker 1973 Radiaxial fibrous calcite: a replacement after acicular carbonate – Sedimentology 20: 365–389

Lippmann, F. 1955 Ton, Geoden und Minerale des Barreme von Hoheneggelsen – Geol. Rundschau 43: 475–503

Marshall, J.D. 1982 Isotopic composition of displacive fibrous calcite veins: reversals in pore water composition trends during burial diagenesis – J. Sedim. Petrol. 52: 615–630

McCrea, J.M. 1950 On the isotopic chemistry of carbonates and paleotemperature scale – J. Chemical Physics 18: 849–857

Moore, S.E., R.E. Ferrell Jr. & P. Aharon 1992 Diagenetic siderite and other ferroan carbonates in a modern subsiding marsh sequence – J. Sedim. Petrol. 62: 357–366

Mortimer, R.J.G. & M.L. Coleman 1997 Microbial influence on the oxygen isotopic composition of diagenetic siderite – Geochim. Cosmochim. Acta 61: 1705–1711.

Mostefaï, S. 1996 Les concrétions septariennes barytiques et carbonatées des marnes bleues du Crétacé (Sud-est de la France) – Unpubl. PhD thesis, Ecole Nationale Sup. Mines, Paris, 315 pp

Mozley, P.S. 1989 Complex compositional zonation in concretionary siderite: implications for geochemical studies – J. Sedim. Petrol. 59: 815–818

Mozley, P.S. & S.J. Burns 1993 Oxygen and carbon isotopic composition of marine carbonate concretions: an overview – J. Sedim. Petrol. 63: 73–83

Pearson, M.J. 1979 Geochemistry of the Hepworth Carboniferous sediment sequence and origin of the diagenetic iron minerals and concretions – Geochim. Cosmochim. Acta 43: 927–941

Raiswell, R. 1971 The growth of Cambrian and Liassic concretions – Sedimentology 17: 147–171

Raiswell, R. 1976 The microbiological formation of carbonate concretions in the Upper Lias of NE England – Chemical Geol. 18: 227–244

Raiswell, R. 1987 Non-steady state microbiological diagenesis and the origin of concretions and nodular limestones. In: Marshall, J.D. (ed.) Diagenesis of Sedimentary Sequences. Geol. Soc. Spec. Publ. 36: 41–54

Raiswell, R. 1988 Chemical model for the origin of minor limestone-shale cycles by anaerobic methane oxidation – Geology 16: 641–644

Richardson, W.A. 1919 On the origin of septarian structure – Min. Mag. Lond. 18: 327–382

Sass, E., A. Bein & A. Almogi-Labin 1991 Oxygen-isotope composition of diagenetic calcite in organic-rich rocks: Evidence for ^{18}O depletion in marine anaerobic pore water – Geology 19: 839–842

Scotchman, I.C. 1991 The geochemistry of concretions from the Kimmeridge Clay Formation of southern and eastern England – Sedimentology 38: 79–106

Shackleton, N.J. 1986 Paleogene stable isotope events – Palaeogeogr., Palaeoclim., Palaeoecol. 57: 91–102

Thyne, G.D. & J.R. Boles 1989 Isotopic evidence for origin of the Moeraki septarian concretions, New Zealand – J. Sedim. Petrol. 59: 272–279

Vandenberghe, N. 1978 Sedimentology of the Boom clay (Rupelian) in Belgium – Verh. Kon. Acad. Wet. België, Kl. Wet., XL, 147, 137 pp

Vandenberghe, N. & P. Laga 1986 The septaria of the Boom clay (Rupelian) in the type area in Belgium – Aardk. Meded. 3: 229–238

Vandenberghe, N., P. Laga, E. Steurbaut, J. Hardenbol & P. Vail (in press) Sequence Stratigraphy of the Tertiary at the southern border of the North Sea basin in Belgium. In: De Graciansky, P.Ch., J. Hardenbol, T. Jacquin, P.R. Vail & M.B. Farley (eds) Mesozoic-Cenozoic Sequence Stratigraphy of Western European Basins – Soc. Econ. Paleontol. Mineral., spec. publ. 60

Van Echelpoel, E. 1991 Kwantitatieve cyclostratigrafie van de formatie van Boom (Rupeliaan – België) – De methodologie van het onderzoek van sedimentaire cycli via Walshanalyse – Unpubl. PhD thesis, K.U. Leuven, 164 pp

Van Echelpoel, E. & G.P. Weedon 1990 Milankovitch cyclicity and the Boom Clay Formation: an Oligocene siliciclastic shelf sequence in Belgium – Geol. Mag. 127: 599–604

Veizer, J. 1992 Depositional and diagenetic history of limestones: stable and radiogenic isotopes. In: Clauer N. & S. Chaudhuri (eds) Isotopic Signatures and Sedimentary Records. Springer Verlag, Berlin: 13–48

Vinken, R. 1988 The Northwest European Tertiary Basin – Geol. Jahrb., Reihe A, Heft 100, Map Nr. 4.

Winter, B.L. & L.P. Knauth 1992 Stable isotope geochemistry of early Proterozoic carbonate concretions in the Animikie Group of the Lake Superior region: evidence for anaerobic bacterial processes – Precambrian Res. 54: 131–151

Zimmerle, W. 1991 Thin-section Petrography of Argillaceous Rocks – Zentralbl. Geol. Paläontol. 1: 365–390

Zimmerle, W. 1993 On the lithology and provenance of the Rupelian Boom Clay in Northern Belgium, a volcanoclastic sediment – Bull. Soc. belge Géol. 102: 91–103